

Learning and Prediction of the Nonlinear Dynamics of Biological Neurons with Support Vector Machines

Thomas Frontzek, Thomas Navin Lal, Rolf Eckmiller

Department of Computer Science VI, University of Bonn
Römerstraße 164, D 53117 Bonn, F. R. Germany
E-mail: {frontzek,lal,eckmiller}@nero.uni-bonn.de

Abstract. Based on biological data we examine the ability of Support Vector Machines (SVMs) with gaussian kernels to learn and predict the nonlinear dynamics of single biological neurons. We show that SVMs for regression learn the dynamics of the pyloric dilator neuron of the australian crayfish, and we determine the optimal SVM parameters with regard to the test error. Compared to conventional RBF networks, SVMs learned faster and performed a better iterated one-step-ahead prediction with regard to training and test error. From a biological point of view SVMs are especially better in predicting the most important part of the dynamics, where the membranepotential is driven by superimposed synaptic inputs to the threshold for the oscillatory peak.

1 Introduction

Modeling on the basis of biological data extracted via intracellular recording is still a challenging task. A biological neural network well studied by physiologists is the stomatogastric ganglion (STG) of crayfish. This neural network consists of a manageable number of specifiable individual neurons. In the literature the dynamics of single neurons or small parts of the STG is modeled on different levels of detail [2]. On the most detailed level ion channels of the membrane of individual neurons are considered for conductance-based Hodgkin-Huxley-models [1]. So called "neuronal caricatures" are on a more abstract level. Here, the dynamics of a neuron are reduced to a few differential equations. Coupled simple binary neurons build the other end of the modeling hierarchy.

Within our paper we focus on the measured time series of specified individual neurons of the STG to model its dynamics. Former studies show that the Support Vector Machine (SVM) technique is very well suited for learning and predicting nonlinear time series. Applied to different benchmarks SVMs perform better than established regression techniques [3] [4]. In contrast to those approaches we apply SVMs to biological data and compare the results generated by our SVMs with the results of conventional RBF networks.

2 The stomatogastric ganglion of crayfish

The stomatogastric ganglion (STG) of crayfish is a model system for biological neural networks. A manageable number of specifiable individual neurons generates several rhythmic motor patterns. The STG consists of the gastric network,

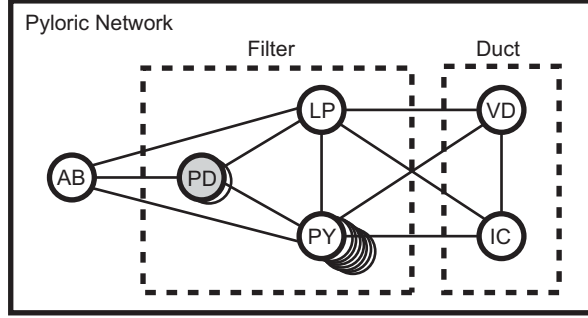


Fig. 1. Pyloric network of crayfish. This network consists of 14 cells: 13 motor neurons of five different cell types (two PD, eight PY, LP, VD, IC) and one interneuron (AB). The synaptic connections are illustrated schematically. Within our paper we focus on the activity of the pyloric dilator (PD) neuron.

which controls the movement of the gastric teeth, and the pyloric network (see fig.1), which controls the movement of the pyloric filter and the cardiopyloric duct.

The pyloric rhythm is driven by the anterior burster (AB) interneuron, which is able to oscillate autonomously. Three phases of the pyloric rhythm can be distinguished: pyloric dilator (PD) neuron, lateral pyloric (LP) neuron, and pyloric (PY) neuron. These neurons are connected with electrical and (mostly inhibitory) chemical synapses.

One can measure the activity of the pyloric network neurons in two different ways: either potentials of single neurons via intracellular recording, or the sum potential of PD, LP and PY via extracellular recording at the dorsal ventricular nerve (dvn). Within our paper we focus on the intracellular measured activity of the PD neuron (see fig.2).

3 Learning and predicting time series with SVMs

Let T be some time series that is generated by an unknown mapping $f : \mathbb{N} \rightarrow \mathbb{R}^d$:

$$T = (f(1), f(2), \dots, f(n)) =: (x_1, x_2, \dots, x_n).$$

Often there is no or little information available about f , so x_{n+1} can only be determined by the information included in T . One common approach is:

1. choose $m, h \in \mathbb{N}$ and a set $L \subseteq \{1, \dots, n\}$,
2. build training data:

$$D = \{((x_{i-mh}, \dots, x_{i-2h}, x_{i-h}), x_i) \in \mathbb{R}^{md} \times \mathbb{R}^d \mid i \in L\},$$
3. choose a class of functions $\mathcal{F} := \{f : \mathbb{R}^{md} \rightarrow \mathbb{R}^d\}$, and then
4. try to find a minimizer \hat{f} of $I : \mathcal{F} \rightarrow \mathbb{R}$, $I[f] := \sum_{(x,y) \in D} V(y, f(x))$ with some appropriate loss function V ,
5. set $\tilde{x}_{n+1} := \hat{f}(x_{n+1-mh}, \dots, x_{n+1-2h}, x_{n+1-h})$.

Minimizing I using SVMs with the ϵ -insensitive loss function:

$$V(y, f(x)) := \begin{cases} 0, & \text{if } |y - f(x)| \leq \epsilon, \\ |y - f(x)| - \epsilon, & \text{otherwise.} \end{cases}$$

leads to the quadratic minimization problem:

$$\min_{\alpha, \alpha^* \in A_\lambda} \left\{ \frac{1}{2} \sum_{i,j=1}^{|L|} (\alpha_i^* - \alpha_i) (\alpha_j^* - \alpha_j) K(x_i, x_j) - \sum_{i=1}^{|L|} \alpha_i^* (y_i - \epsilon) - \alpha_i (y_i + \epsilon) \right\}$$

with $K : \mathbb{R}^{2d} \rightarrow \mathbb{R}$ satisfying the Mercer-condition, $\sum_{i=1}^{|L|} (\alpha_i^* - \alpha_i) = 0$, $A_\lambda := \{\alpha \in \mathbb{R}^{|L|} : 0 \leq \alpha_i \leq \frac{1}{\lambda}, 1 \leq i \leq |L|\}$, (λ regularization parameter), which is equivalent to

$$\min_{\beta \in \mathbb{R}^{2|L|}} \left\{ -c^t \beta + \frac{1}{2} \beta^t H \beta \right\}, \quad \text{with } A\beta = b, l \leq \beta \leq u.$$

The matrix H consists of pairwise scalar products of the input data in the feature space:

$$H = \begin{pmatrix} \vdots & & \vdots \\ \dots + K(x_i, x_j) & \dots & -K(x_i, x_j) \dots \\ \vdots & & \vdots \\ \vdots & & \vdots \\ \vdots & & \vdots \\ \dots -K(x_i, x_j) & \dots & +K(x_i, x_j) \dots \\ \vdots & & \vdots \end{pmatrix}, \quad c = \begin{pmatrix} -y_1 - \epsilon \\ \vdots \\ -y_{|L|} - \epsilon \\ +y_1 - \epsilon \\ \vdots \\ +y_{|L|} - \epsilon \end{pmatrix}.$$

The vector β is defined as:

$$\beta = \begin{pmatrix} \alpha_1 \\ \vdots \\ \alpha_{|L|} \\ \alpha_1^* \\ \vdots \\ \alpha_{|L|}^* \end{pmatrix}, \quad A = \begin{pmatrix} 1 \\ \vdots \\ 1 \\ -1 \\ \vdots \\ -1 \end{pmatrix}, \quad b = 0, \quad l = 0, \quad u = \frac{1}{\lambda} \begin{pmatrix} 1 \\ \vdots \\ 1 \end{pmatrix}, (x_i, y_i) \in T.$$

4 Results

4.1 Biological data

We used data from the pyloric network of the australian crayfish *cherax destructor albidus*. The intracellular recordings were done using glass-microelectrodes, filled with $3MKCl$ solution and with resistors ranging from $16M\Omega$ to $25M\Omega$. The data was recorded with an A-D-converter and a video-8-recorder¹.

To reduce the amount of data we replaced every 1000 consecutive datapoints by their average. Then we scaled the results to fit into $[-0.9, 0.9]$. Our training

¹ Recordings were provided by G. Heinzel, H. Böhm, C. Gutzen, Department of Neurobiology, University of Bonn.

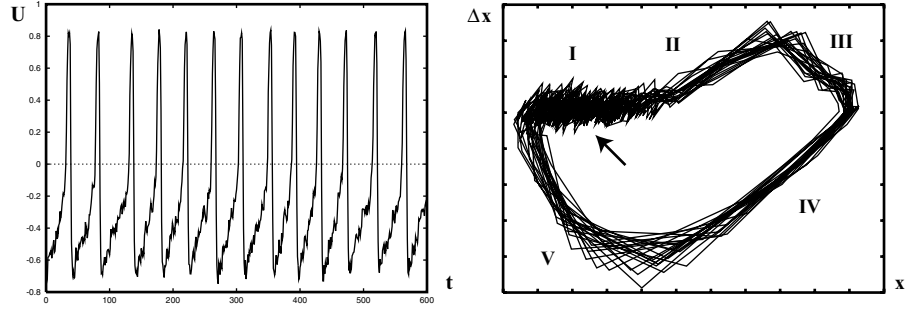


Fig. 2. Time series of the pyloric dilator neuron (left), and phase portrait of its dynamics (right). One can distinguish five sections within the phase portrait, marked I to V. Section I is most important, because here the membranpotential is driven by superimposed synaptic inputs to the threshold for the oscillatory peak (sections II to V).

set consisted of 200 patterns (patterns 21 – 220 of fig.2) and the test set of 100 patterns (patterns 221 – 320 of fig.2). For our iterated one-step-ahead prediction we wanted to learn the dynamics of the given time series from the last 20 data points and we therefore set $m = 20$, $h = 1$, and $L = \{21, 22, \dots, 220\}$.

To test the generalization ability of our approximator A (SVM or RBF), which was trained to learn the data $(x_{21}, x_{22}, \dots, x_{220})$, we recursively set

$$\begin{aligned} \tilde{x}_i &:= x_i, & i &= 1..20 \\ \tilde{x}_{20+i} &:= A(\tilde{x}_{(20+i)-20}, \tilde{x}_{(20+i)-19}, \dots, \tilde{x}_{(20+i)-1}), & i &= 1..300 \end{aligned}$$

and then calculated the test error

$$E[A] := \frac{1}{100} \sum_{i=221}^{320} |\tilde{x}_i - x_i|. \quad (1)$$

4.2 Simulations with Support Vector Machines

We adapted the *LOQO* algorithm by Vanderbei [5] which was implemented by Smola and set the regularization parameter to $\lambda = 0.05$.

Varying the variance σ from 0.05 to 100 and the exactness ϵ from 0.001 to 0.8 we performed a large number of simulations. After the learning process we calculated the training and test errors (see equation 1). Fig.3 shows the test error for the most interesting area, which is $\sigma = [0.05, 3.0]$ and $\epsilon = [0.001, 0.01]$.

One can observe a valley of low error values as well as several peaks of very low error values for certain combinations of σ and ϵ .

Regarding the test error the best SVM we found was SVM_{best} with $\sigma = 2.85$ and $\epsilon = 0.04$. SVM_{best} used 196 support vectors and had a test error of 0.04622. Fig.4 shows the predicted values of SVM_{best} compared to the original values.

We also performed simulations using other than the gaussian kernel. As we expected *tanh*-kernels and polynomial kernels showed worse results. This could be explained by the more global properties of those functions.

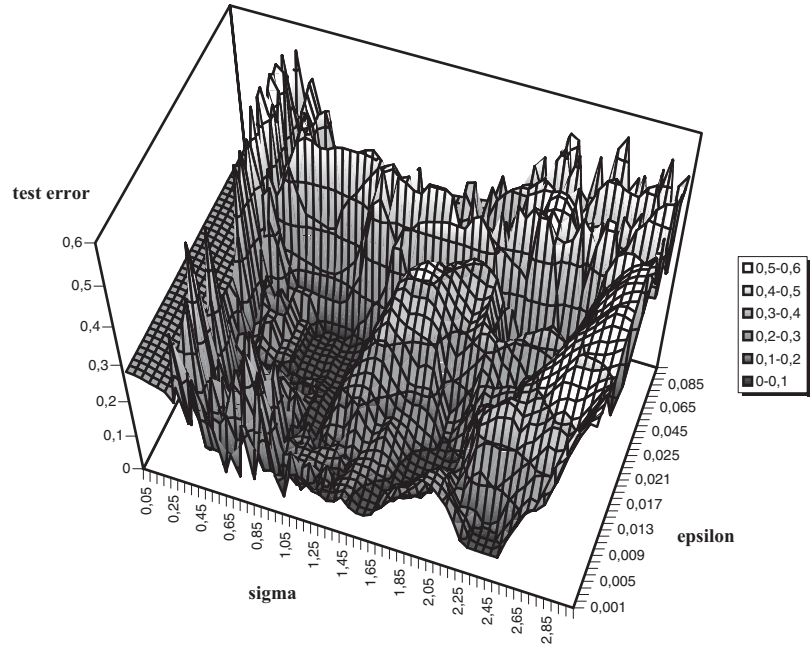


Fig. 3. Test error of SVM with gaussian kernel subject to variance σ and exactness ϵ . One can observe a valley of low error values as well as several peaks of very low error values for certain combinations of σ and ϵ .

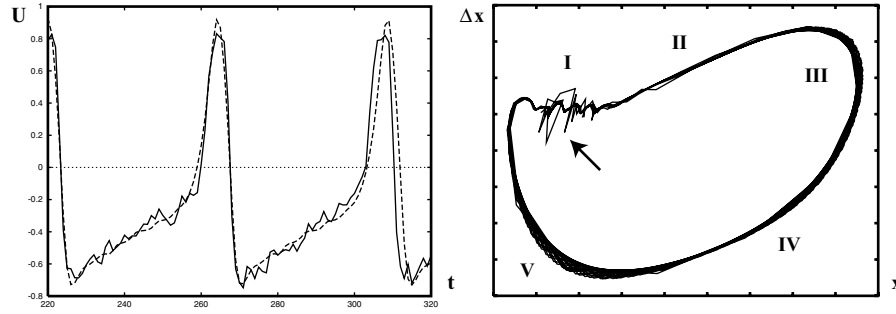


Fig. 4. Iterated one-step-ahead prediction of the PD time series (solid line) with SVM_{best} (dashed line)(left), and phase portrait of the corresponding dynamics (right). Parameters of SVM_{best} are: $\sigma = 2.85$, $\epsilon = 0.04$, number of support vectors = 196. Primarily the increasing sections ($t = [230, 250]$ and $t = [275, 295]$) resp. section I of the phase portrait are predicted better than those predicted by RBF_{best} (see fig.6).

4.3 Simulations with RBF networks

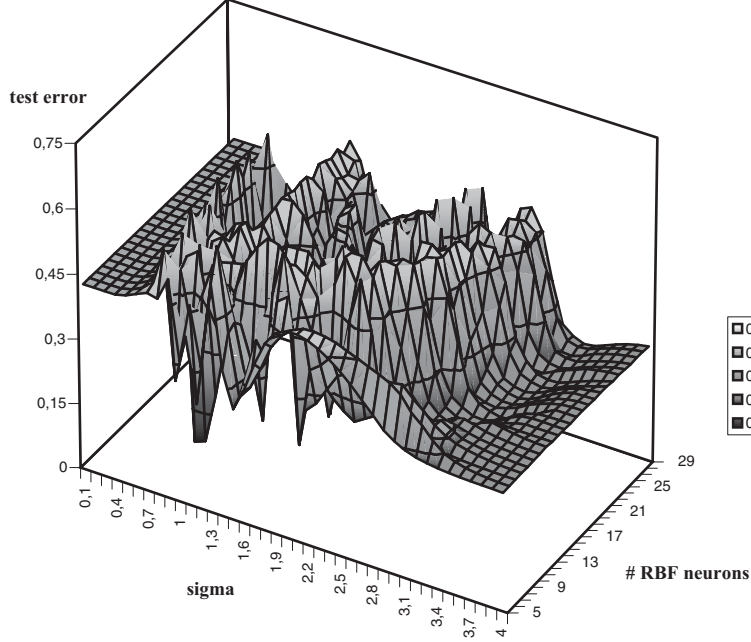


Fig. 5. Test error of RBF network subject to variance σ and the number of RBF neurons. The landscape of test error has two plateaus, one with $\sigma < 0.5$ and one with $\sigma > 3.5$. In between one can observe some mountain ranges of high error values as well as several peaks of very low error values.

In a first step the centers of the RBF neurons were determined by a *k-means-clustering* algorithm for a given k . The weights of the output layer were set randomly in $[-0.0001, 0.0001]$. Then, in a second step these weights were learned using the delta rule. We stopped the learning process when the change of error was less than 10^4 for the last 20 epochs, compared to the actual epoch.

Varying the variance σ from 0.1 to 100 and the number of RBF neurons from 5 to 200 we again performed a large number of simulations. After the learning process we calculated the training and test errors (see equation 1). Fig. 5 shows the test error for the most interesting area, which is $\sigma = [0.1, 4.0]$ and number of RBF neurons $= [5, 29]$.

The landscape of test error has two plateaus, one with $\sigma < 0.5$ and one with $\sigma > 3.5$. In between one can observe some mountain ranges of high error values as well as several peaks of very low error values.

Regarding the test error the best RBF network we found was RBF_{best} with 26 RBF neurons and $\sigma = 0.7$. RBF_{best} had a test error of 0.07295. Fig. 6 shows the predicted values of RBF_{best} compared to the original values. Primarily the increasing sections ($t = [230, 250]$ and $t = [275, 295]$) are predicted worse than those predicted by SVM_{best} (see fig. 4), whereas the oscillatory peak (sections II to V of the phase portrait) is predicted better by RBF_{best} (see fig. 6).

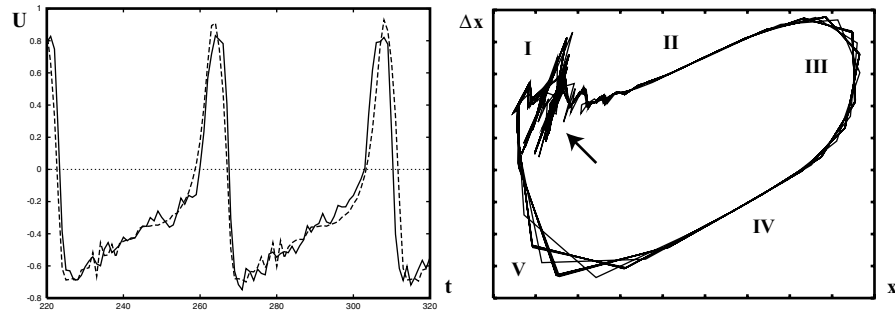


Fig. 6. Iterated one-step-ahead prediction of the PD time series (solid line) with RBF_{best} (dashed line) (left), and phase portrait of the corresponding dynamics (right). Parameters of RBF_{best} are: $\sigma = 0.7$, number of RBF neurons = 26. Primarily the increasing sections ($t = [230, 250]$ and $t = [275, 295]$) resp. section I of the phase portrait are predicted worse than those predicted by SVM_{best} (see fig. 4), whereas the oscillatory peak (sections II to V of the phase portrait) is predicted better by RBF_{best}.

4.4 Comparison of the SVM and RBF results

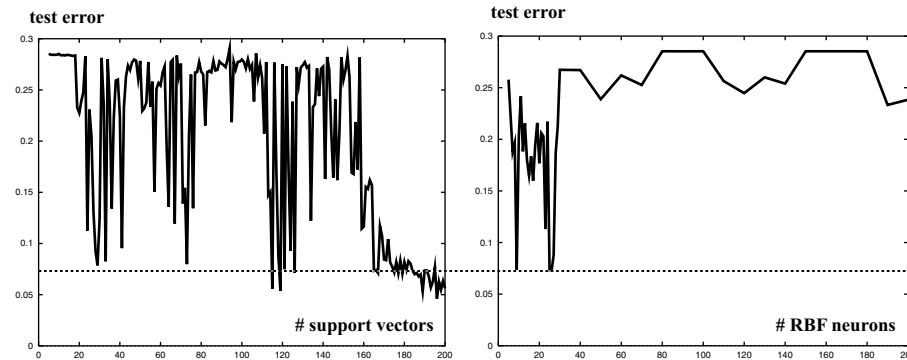


Fig. 7. Test error subject to the number of support vectors (left) and the number of RBF neurons (right). For every number of support vectors resp. RBF neurons we plotted the lowest test error that was achieved by the corresponding network.

The results of the previous sections showed that SVMs obtained lower test errors than RBF networks, leading to better predictions. For further comparison we examined the test error subject to the number of support vectors resp. the number of RBF neurons. In fig. 7 we plotted for every number of support vectors resp. RBF neurons the lowest test error that was achieved by the corresponding network. Best results for SVMs were obtained using a large number of support vectors (compared to the number of training patterns), whereas best results for RBF networks were obtained using few RBF neurons. Nevertheless, SVMs with about 115 support vectors and even SVMs with about 25 support vectors had test errors which were as low as those of RBF_{best}.

The following table summarizes our results for the lowest training error, test error and the sum of training and test error. It also shows the learning times (using a Pentium-III computer with 700MHz speed and 128MBytes memory) of the listed networks. All SVMs learned much faster than the corresponding RBF networks.

	SVM (# support vectors)	RBF (# RBF neurons)
best training error	0.02752 (200)	0.17105 (18)
best test error	0.04622 (196)	0.07295 (26)
best error sum	0.19868 (198)	0.33106 (09)
learning times [s]	15/15/15	309/93/27

From a biological point of view SVMs were especially better in predicting the most important part of the dynamics, where the membranpotential is driven by superimposed synaptic inputs to the threshold for the oscillatory peak, whereas RBF networks were better in predicting the different sections of the oscillatory peak.

5 Conclusions

On the basis of the results of our large number of simulations we conclude:

- SVMs for regression were able to learn the nonlinear dynamics of biological data. This was demonstrated with the dynamics of the pyloric dilator neuron of the crayfish *cherax destructor albidus*.
- Compared to conventional RBF networks SVMs with gaussian kernels performed a better iterated one-step-ahead prediction with regard to training and test error. SVMs were especially better in predicting the most important part of the dynamics, where the membranpotential is driven by superimposed synaptic inputs to the threshold for the oscillatory peak.
- SVMs learned faster than RBF networks.
- Best results for SVMs were obtained using a large number of support vectors (compared to the number of training patterns), whereas best results for RBF networks were obtained using few RBF neurons.

Acknowledgments

Parts of this work have been supported by the Federal Ministry for Education, Science, Research, and Technology (BMBF), project LENI. Thanks to Hartmut Böhm and Mikio L. Braun for useful comments.

References

1. Jorge Golowasch, Michael Casey, L. F. Abbott, and Eve Marder. Network stability from activity-dependent regulation of neuronal conductances. *Neural Computation*, (11):1079–1096, 1999.
2. Eve Marder and Allen I. Selverston. Modeling the stomatogastric nervous system. In Ronald M. Harris-Warrick, Eve Marder, Allen I. Selverston, and Maurice Moulins, editors, *Dynamic Biological Networks*, pages 161–196. The MIT Press, 1992.
3. K.-R. Müller, A. J. Smola, G. Rätsch, B. Schölkopf, J. Kohlmorgen, and V. Vapnik. Predicting time series with support vector machines. In *Proceedings of ICANN'97, Lausanne*, pages 999–1004, 1997.
4. Sayan Mukherjee, Edgar Osuna, and Federico Girosi. Nonlinear prediction of chaotic time series using support vector machines. In *Proceedings of IEEE NNISP'97*, pages 511–519, 1997.
5. Robert J. Vanderbei. *LOQO: An Interior Point Code for Quadratic Programming*. Technical Report SOR94-15. Princeton University, 1994.